


# Angular momentum distribution of atomic hydrogen in excited states under ultra-short laser field

Zhaoyan Zhou(周兆妍)†, Dongwen Zhang(张栋文), and Zengxiu Zhao(赵增秀)

**Citation:**Chin. Phys. B, 2026, 35 (**3**): 033201. DOI: 10.1088/1674-1056/adfdc6
http://cpb.iphy.ac.cn; http://iopscience.iop.org/cpb

**What follows is a list of articles you may be interested in**

---

## Semiclassical Coulomb-scattering model for strong-field tunneling ionization

Qing Zhao(赵晴), Yigen Peng(彭易根), Jiayin Che(车佳殷), Chao Chen(陈超), Shang Wang(王赏), Guoguo Xin(辛国国), and Yanjun Chen(陈彦军)
Chin. Phys. B, 2025, 34 (**9**): 093201. DOI: 10.1088/1674-1056/ade06e

## Theory and applications of attosecond transient absorption spectroscopy: From atoms to solids

Ennan Cui and Difa Ye(叶地发)
Chin. Phys. B, 2025, 34 (**7**): 073201. DOI: 10.1088/1674-1056/add1ba

## Theoretical investigations of population trapping phenomena in atomic four-color, three-step photoionization scheme

Xiao-Yong Lu(卢肖勇) and Ya-Peng Sun(孙亚鹏)
Chin. Phys. B, 2024, 33 (**3**): 033202. DOI: 10.1088/1674-1056/ad10fc

## Influence of acceleration on relativistic nonlinear Thomson scattering in tightly focused linearly polarized laser pulses

Yifan Chang(常一凡), Yubo Wang(王禹博), Chang Wang(王畅), Yuting Shen(申雨婷), and Youwei Tian(田友伟)
Chin. Phys. B, 2023, 32 (**6**): 063201. DOI: 10.1088/1674-1056/ac89e6

## Asymmetry parameters in single ionization of He, Ne by XUV pulses

Jian-Ting Lei(雷建廷), Xuan Yu(余璇), Guo-Qiang Shi(史国强), Chen-Yu Tao(陶琛玉), Shao-Hua Sun(孙少华), Shun-Cheng Yan(闫顺成), Xin-Wen Ma(马新文), Jing-Jie Ding(丁晶洁), and Shao-Feng Zhang(张少锋)
Chin. Phys. B, 2023, 32 (**5**): 053205. DOI: 10.1088/1674-1056/aca6d9

---

# Angular momentum distribution of atomic hydrogen in excited states under ultra-short laser field

Zhaoyan Zhou(周兆妍)†, Dongwen Zhang(张栋文), and Zengxiu Zhao(赵增秀)

*Department of Physics, College of Science, National University of Defense Technology, Changsha* 410073, *China*

(Received 10 June 2025; revised manuscript received 10 August 2025; accepted manuscript online 21 August 2025)

We investigate the population distribution of excited angular momentum ($l$) states in the interaction between a hydrogen atom and an ultra-short laser pulse. Through numerical solution of the time-dependent Schrödinger equation, we theoretically investigate the laser-induced oscillations among excited $l$-states. Temporal evolution analysis reveals distinctive signatures of both multiphoton excitation and frustrated tunneling ionization processes. Specifically, multiphoton excitation dominates during the final optical cycle as the laser peak intensity attenuates, thereby critically determining the final $l$-states population distribution. We demonstrate that the angular quantum states' parity effect does not persist, even for ultra-short pulses with broad frequency bandwidths. The parity effect is also unaffected by laser field asymmetry.

**Keywords:** ultra-short laser pulses, excited angular momentum states, time-dependent Schrödinger equation, parity effect

**PACS:** 32.80.–t, 32.80.Rm, 31.70.Hq

**DOI:** 10.1088/1674-1056/adfdc6 **CSTR:** 32038.14.CPB.adfdc6

## 1. Introduction

In the interaction of the atoms and molecules with a strong laser field, the existence of excited states was reported experimentally in the 1990s.[1–3] However, for decades, the underlying physical mechanism and dynamical evolution of these excited states remained poorly understood. This was primarily because the electron dynamics in strong laser field were predominantly associated with ionization, and the population of excited states was considered negligible in comparison. Consequently, excitation processes received limited attention in early studies.

Recently, there were many experiments and theoretical calculations showing that the population of excited neutral atoms in a strong laser field is not negligible.[4,5] These observations caused interest in understanding the underlying mechanisms of electron trapping in excited states. For atoms in a strong laser field, ionization is typically described by two regimes: multiphoton ionization (MPI) and tunneling ionization (TI).[6–8] The regimes are characterized by the Keldysh parameter $\gamma = (I_p/2U_p)^{1/2}$,[9] where $I_p$ denotes the ionization potential and $U_p$ represents the ponderomotive energy of the laser field. Building on these fundamental ionization regimes, researchers have proposed two models for the population of excited states.

When $\gamma \gg 1$, MPI dominates and the electron can be ionized via the absorption of multiple photons. Within this regime, the electron can also be resonant excited to ac-Stark-shifted excited states via multiphoton absorption. Li *et al.*[10,11] proposed the channel-closing effect based on the MPI model through numerical solutions of the time-dependent Schrödinger equation (TDSE). This effect successfully explains the periodic dependence of the total excited-state population on laser intensity. Subsequent experiments[12–14] have confirmed their theoretical simulation results.

For $\gamma \ll 1$, TI becomes important and the electron dynamics in a strong laser field can be effectively described by the classical three-step rescattering model.[15] In this model, the electron can be first ionized via TI and then accelerated by the laser field. When the laser field reverses direction, the electron can be driven back to recollide with its parent ion. Many strong-field phenomena such as high-order harmonic generation (HHG), high-energy above-threshold (HATI) and nonsequential double ionization (NSDI) can be effectively described by the three-step model. A common feature of these phenomena is their dependence on laser ellipticity, which significantly affects the recollision probability and, consequently, their yields. Both theoretical and experimental studies[5,16–19] have also demonstrated that the population of excited neutral atoms decreases dramatically with increasing laser ellipticity. This observation motivated researchers to incorporate the excitation process into the three-step model, and thus the frustrated tunneling ionization (FTI) model was proposed.[5,20] In this model, tunnel-ionized electrons can be recaptured into excited states when they are driven back to the vicinity of its parent ion.

The population distribution of the principal quantum number $n$ is often explained within the TI regime: the most probable $n$-state corresponds to an electron orbital radius ($r \propto$

†Corresponding author. E-mail: cnzhzhy@nudt.edu.cn

© 2026 Chinese Physical Society and IOP Publishing Ltd. All rights, including for text and data mining, AI training, and similar technologies, are reserved.

$n^2$) matching the classical quiver radius ($r = F/\omega^2$) of the electron in strong laser field characterized by amplitude $F$ and frequency $\omega$.[5,21] This correspondence between quantum mechanical states and classical electron motion helps roughly estimate the $n$-state population in a strong laser field.

The population distribution of angular momentum states ($l$-states) has also attracted significant research attention, and it exhibits a complex dependence on laser parameters.[22–25] Venzke *et al.*[22] introduced the parity effect, i.e., the parity of the angular momentum quantum number $l$ of the occupied excited states matches the parity of the minimum photon number required for ionization. However, the parity effect breaks down for an ultrashort laser pulses due to their broad bandwidth. Chetty *et al.*[23,24] explored the influence of the carrier envelop phase (CEP) of ultrashort laser pulses on the population of excited $l$-states. Their results demonstrate that the parity effect persists at CEP = 0, and breaks down for CEP = $0.5\pi$ when the laser intensity is sufficiently high to reach the TI regime. They attributed this breakdown of parity effect to the spatial asymmetry of laser field, while the detailed physical mechanism was not fully discussed.

In this paper, we focus on the excitation process to different $l$-states in the interaction between a hydrogen atom and ultrashort laser field. We explore the population distributions of excited $l$-states for different laser intensities and CEPs. This study aims to identify the dominant excitation mechanism governing the $l$-state population and find out the role of laser field asymmetry in determining $l$-state distributions as well as the parity effect.

## 2. Theoretical methods

We calculate the evolution of the wavepacket in a strong laser field by carrying out the numerical solution of the TDSE (in atomic units)

$$\mathrm{i}\frac{\partial}{\partial t}\psi(\boldsymbol{r},t) = (\hat{H}_0 + \hat{H}_\mathrm{I})\psi(\boldsymbol{r},t), \tag{1}$$

where $\hat{H}_0$ is the field-free Hamiltonian and $\hat{H}_\mathrm{I}$ is the interaction part given in the length gauge. In the dipole approximation,

$$\hat{H}_\mathrm{I} = -\boldsymbol{E}_\mathrm{L}\cdot r f(t)\cos(\omega t + \varphi), \tag{2}$$

where the envelope of the laser pulse, $f(t)$, is chosen to be sine-square form with a few optical cycles (o.c.) duration. $E_\mathrm{L}$ is the amplitude and $\varphi$ is the CEP of laser field. $\omega$ is the frequency and is fixed to be 0.057 a.u. corresponding to a 800 nm laser field.

Linearly polarized laser pulses are considered throughout the investigation, thus we only need to consider the $m = 0$ component of the magnetic quantum number of the atom. The time-dependent wave function is expanded with Legendre polynomials in the $\theta$ coordinate as

$$\psi(r_i,x_j,t) = \sum_{l=0}^{L} c_l(t)R_l(r_i)P_l(x_j), \quad x_j = \cos\theta_j, \tag{3}$$

and the radial function $R_l(r)$ is expanded using a discrete variable representation (DVR) basis set associated with Legendre polynomials.[26–28] The time-dependent coefficients $c_l(t)$ are obtained initially by diagonalizing the field-free Hamiltonian and then calculated using the split-operator method.[29] For numerical implementation, we expand the wave functions with 3500 DVR points for $r_\mathrm{max} = 1500$ a.u. and 120 partial waves to ensure convergence of the results.

## 3. Results and discussion

We begin by examining the excited-states population distribution for laser intensity $I_\mathrm{L} = 1.4\times10^{14}$ W/cm$^2$ with different CEPs $\varphi$. For $\varphi = 0$, the electron predominantly occupies the $l = 4$ excited state as shown in Fig. 1(a). The secondary population maximum is $l = 2$, consistent with the parity effect.[22,24] A more detailed analysis in Fig. 1(b) reveals the (5,4) state as the most populated. However, the parity effect is not always evident and the occupation of the excited states is more complex when the CEP changes, as shown in Figs. 1(c)–1(e). These simulation results are consistent with the work of Chetty *et al.*,[24] who attributed the breakdown of the parity effect to the asymmetry of the laser field. For $\varphi = 0.5\pi$ when the laser field is the most asymmetric, the electron is predominantly trapped in the (6,5) state. The electron can be excited to $l = 4$ and 5 states without following the parity effect, as shown in Fig. 1(a).

To further investigate the influence of laser field asymmetry on the distribution of excited $l$-states, we then make more calculations for different laser intensities focusing on $\varphi = 0$ and $0.5\pi$. Our results reveal that even at $\varphi = 0$, the parity effect is not consistently observed as the laser intensity varies, as shown in Fig. 2(a). In addition, the electron population distribution for $\varphi = 0.5\pi$ (Fig. 2(b)) consistently shows broader $l$-state occupation compared to $\varphi = 0$, regardless of whether the system is in the MPI or TI regime. How different CEPs influence $l$-state population distributions and the underlying electron dynamics is the key issue we aim to address next.

Given that the energy levels are significantly altered by the ac-Stark-shift, it is hard to accurately track the temporal population oscillation of a specific quantum state in the presence of strong laser field. Therefore, we instead analyze the temporal evolution of a specific angular momentum state. Since the time-dependent wave function is expanded in terms of Legendre polynomials here, we can conveniently obtain the temporal oscillation of electron partial waves with fixed $l$. Figure 3 presents the temporal oscillations of the $l = 2,3,4,5$

states for $\varphi = 0$ and $0.5\pi$. These simulation results focus on the $l$-state distribution of the entire electron wave packet rather than a specific quantum state. Because the photon absorption or emission processes can be more effectively characterized by $l$, this representation can provide clearer insight into the fundamental excitation mechanisms of the electron in a strong laser field.

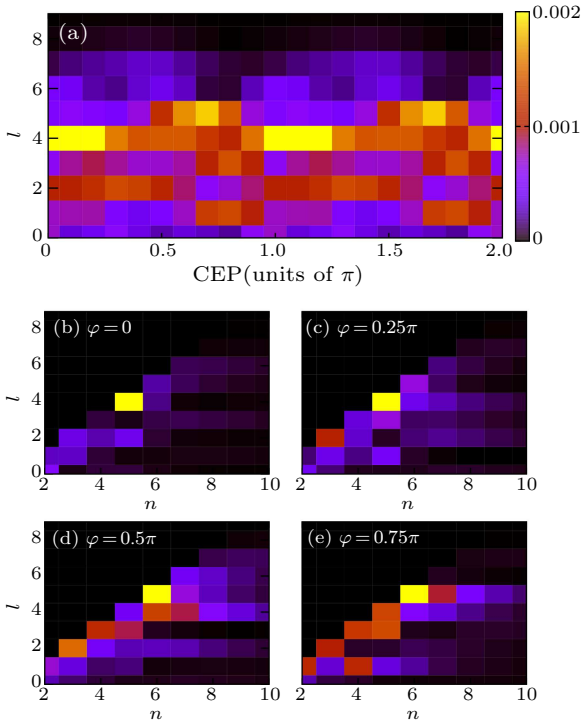



**Fig. 1.** (a) The CEP $\varphi$-dependent population distribution of the excited $l$-states for atomic hydrogen at the end of the 4 o.c. 800 nm laser pulse at fixed intensity $I_L = 1.4 \times 10^{14}$ W/cm$^2$. The corresponding distribution as a function of the principal quantum number $n$ (horizontal axis) and the angular quantum number $l$ (vertical axis) is shown in (b) for $\varphi = 0$, (c) for $\varphi = 0.25\pi$, (d) for $\varphi = 0.5\pi$ and (e) for $\varphi = 0.75\pi$.

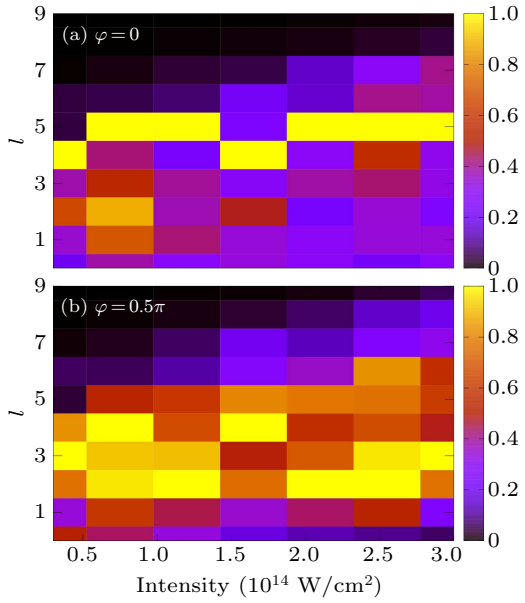



**Fig. 2.** Normalized probability distributions of excited $l$-states across laser intensities for two CEPs: (a) $\varphi = 0$ and (b) $\varphi = 0.5\pi$.

For $\varphi = 0$ in Fig. 3(a), during the first optical cycle in the rising part of the laser field, the laser intensity is insufficient to excite the electron to $l \geq 2$ states. As the field peak intensity increases ($-0.75$ o.c. $< t < 0$, labeled '1'), the electrons are gradually excited to higher $l$-states through photon absorption. This behavior is consistent with the MPI model. Following this, the population of the $l$-states begins to oscillate (labeled '2'). We attribute this oscillation to the recollision process, i.e., electrons ionized in the previous half optical cycle may be driven back to the parent ionic core, inducing rapid population transfer between adjacent states. This recollision-mediated excitation mechanism is in accordance with the FTI model.

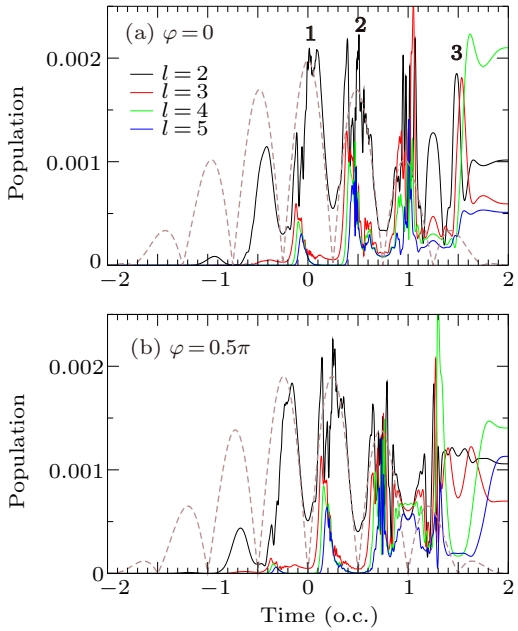



**Fig. 3.** The temporal evolution of the $l$-state population for (a) $\varphi = 0$ and (b) $\varphi = 0.5\pi$. The brown dashed line indicates the variation of the absolute value of the laser field (divided by 32 for clearer visualization of its magnitude). The laser parameters are the same as those in Fig. 1.

As the population of recaptured electrons increases with the increasing laser peak intensity, the oscillation between $l$-states becomes more pronounced. During 0.25 o.c. $< t <$ 1.25 o.c., electronic states with opposite parity exhibit anti-phase oscillations by exchanging photons. However, this phenomenon diminishes before the laser field terminates. In the subsequent decreasing part of the laser field (1.25 o.c. $< t <$ 1.75 o.c.), the probability of the returning electron decreases, and the FTI model is no longer applicable. The $l$-state electron distribution reverts to exhibit multiphoton excitation characteristics, where electrons progressively occupy higher $l$-states through sequential photon absorption (labeled '3'). During this process, the electron is progressively excited to $l = 4$. Then the laser peak intensity is too weak to excite the electron to $l = 5$ and the dominance of the $l = 4$ state continues until the end of the laser pulse.

Compared to the case of $\varphi = 0$, the electric field is shifted by 0.25 o.c. for $\varphi = 0.5\pi$. The $l$-state temporal evolution exhibits similar characteristics to those observed for $\varphi = 0$

when $t < 1.0$ o.c., i.e., the electron is first multiphoton excited and then undergoes FTI to high $l$ states. As stated above, it is not possible to determine which $l$ state dominates at this moment. The key differences emerge in subsequent interactions. During 1 o.c. $< t <$ 1.5 o.c., the $l$-state population again exhibits multiphoton excitation behavior, allowing the electron to absorb photons and be excited to the $l = 5$ state. This occurs at higher laser peak intensity compared to the case when 1.25 o.c. $< t <$ 1.75 o.c. for $\varphi = 0$, and the $l = 4$ and 5 states are both excited. Because these two states have relatively longer lifetimes, fewer transitions are observable between them, and the advantages of $l = 4$ and 5 states are both maintained until the end of the laser pulse. As a result, the electron occupies broader $l$ states for $\varphi = 0.5\pi$ as shown in Fig. 1(a).

As previously discussed, both MPI and FTI play significant roles in the population distribution of excited states. In particular, the shape of the laser pulse near the end of the laser field is crucial in determining the final $l$-states population. When the CEP shifts by $\pi$, the spatial distribution of the laser electric field is inverted, while the temporal evolution of the laser intensity remains unchanged. Consequently, the populations of the excited states remain nearly identical. So, the population distribution of the excited states oscillates periodically with a period of $\pi$, as illustrated in Fig. 1(a). However, it remains uncertain whether the spatial asymmetry of the laser field significantly influences the population distribution of excited states and the parity effect from the preceding discussions.

To further investigate this behavior, we extended the laser duration from 4 o.c. to 4.5 o.c., corresponding to an additional 0.25 o.c. extension in turn-on and turn-off of the laser pulse. In such variations, the asymmetry of the laser field is preserved for a fixed CEP, while the envelope profile of the final optical cycle is altered. The temporal evolution of the $l$-states for $\varphi = 0$ and $0.5\pi$ is illustrated in Fig. 4. Compared with Fig. 3, the $l$-state evolvement remains almost unchanged for $\varphi = 0$ when $t < 1.0$ o.c. and for $\varphi = 0.5\pi$ when $t < 1.25$ o.c.. However, significant differences emerge during the final optical cycle. As the laser envelope decreases more slowly, the corresponding laser peak intensity at the same time is higher than that of the 4 o.c. duration. Multiphoton excitation happens later (1.75 o.c.) for $\varphi = 0.5\pi$ than that for laser duration of 4 o.c. ($t = 1.25$ o.c.), as shown in Fig. 4(b). So, the oscillations between states cannot persist for long. After the electrons being sequentially excited to the $l = 5$ state, its advantage persists until the pulse terminates. This results in a clear occupation of the highest $l = 5$ state, satisfying the conditions for the parity effect. Therefore, the final $l$-state distribution resembles that observed for a 4 o.c. pulse with $\varphi = 0$ discussed before, where the parity effect is also clearly present.

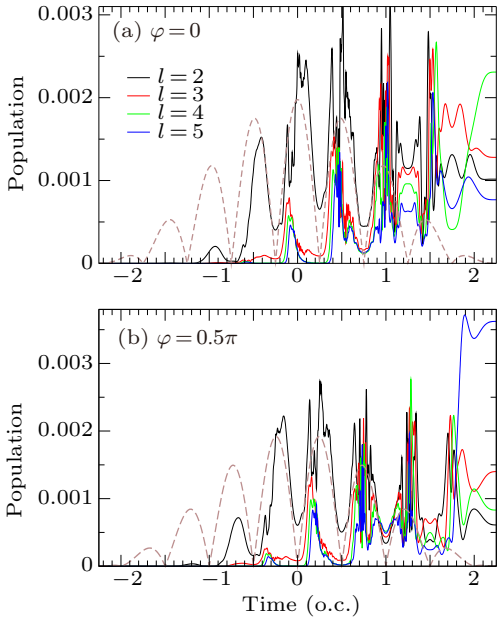



**Fig. 4.** The temporal evolution of the population of $l$-states for (a) $\varphi = 0$ and (b) $\varphi = 0.5\pi$. The brown dashed line indicates the variation of the absolute value of the laser field. Compared to Fig. 3, the laser duration is extended from 4.0 o.c. to 4.5 o.c.

For $\varphi = 0$, the influence of increased laser duration on the population distribution of excited $l$-states is primarily observed when $t > 1.5$ o.c. The electron no longer exhibits a monotonic excitation process toward higher $l$-states, but instead continues to oscillate between adjacent states due to the higher laser peak intensity associated with the extended laser duration as shown in Fig. 4(a). At $t = 1.5$ o.c., the laser field reaches its peak again but remains sufficiently strong to motivate state transitions. The $l = 2$ and $l = 3$ populations exhibit anti-phase oscillations indicating laser-driven transitions between these states. As a result, the second most populated state shifts from $l = 2$ (for 4 o.c. laser duration) to $l = 3$, which is adjacent to the highest occupied state $l = 4$. Consequently, the parity effect is no longer observed.

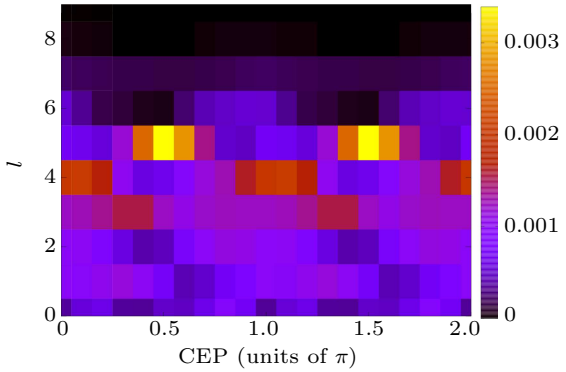



**Fig. 5.** The $\varphi$-dependent probability distribution of excited $l$-states. Compared to Fig. 1, the laser duration is extended from 4 o.c. to 4.5 o.c.

Figure 5 is the $\varphi$-dependent probability distribution of excited $l$-states for a laser duration of 4.5 o.c., which maintains its characteristic $\pi$-periodic dependence on the CEP. However, extending the laser duration by 0.5 o.c. induces significant

modifications compared to Fig. 1. Here the electron population becomes concentrated in states of specific parity when $\varphi$ is around $0.5\pi$, similar to the $\varphi = 0$ case with 4.0 o.c. laser duration. Conversely, the parity effect for $\varphi = 0$ (4 o.c.) disappears when the laser duration is increased by 0.5 o.c. even though the laser duration extension preserves the field's symmetry properties.

These results reveal that pulse duration can serve as an independent control parameter to modulate the parity effect, independent of the field's inherent symmetry properties. After all, strong-field phenomena such as terahertz generation and above-threshold ionization asymmetries, which are known to be sensitive to field asymmetry, remain nearly unchanged with the 0.5 o.c. pulse duration extension. Based on these observations, we challenge the prevailing view that the wide bandwidth of the ultrashort laser pulse and its spatial asymmetry are the key parameters governing both the broad $l$-state distribution and the disappearance of parity effects in Refs. [22,24].

## 4. Conclusions

In this paper, we have explored the dynamics of electrons in atomic hydrogen excited to various $l$-states by ultrashort laser pulses. Our analysis reveals that the evolving laser envelope exposes the electron to varying peak intensities, which alters the excitation mechanism. At relatively weak peak intensities, electrons are multiphoton excited to higher $l$-excited states. At higher peak intensities, electrons experience a rescattering process that induces strong oscillations between excited states, consistent with the FTI model. The coexistence of multiphoton and FTI processes complicates the determination of the dominant electron excitation mechanism in strong laser field.

Our computational simulations reveal that multiphoton excitation dominates during the final cycle of the laser field. At this stage, the envelope shape of the laser pulse becomes the primary factor determining the final $l$-state population distribution, rather than the bandwidth or the spatial asymmetry of the laser field.

## Acknowledgement

Project supported by the National Natural Science Foundation of China (Grant Nos. 12374241 and 12374263).

## References

[1] Muller H G, van Linden van den Heuvell H B, Agostini P, Petite G, Antonetti A, Franco M and Migus A 1988 *Phys. Rev. Lett.* **60** 565

[2] Jones R R, Schumacher D W and Bucksbaum P H 1993 *Phys. Rev. A* **47** R49

[3] Rottke H, Wolf-Rottke B, Feldmann D, Welge K H, Dörr M, Potvliege R M and Shakeshaft R 1994 *Phys. Rev. A* **49** 4837

[4] Wang B, Li X, Fu P, Chen J and Liu J 2006 *Chin. Phys. Lett.* **23** 2729

[5] Nubbemeyer T, Gorling K, Saenz A, Eichmann U and Sandner W 2008 *Phys. Rev. Lett.* **101** 233001

[6] Becker W, Grasbon F, Kopold R, Milošević D B, Paulus G G and Walther H 2002 *Adv. At. Mol. Opt. Phys.* **48** 35

[7] Milošević D B and Ehlotzky F 2003 *Adv. At. Mol. Opt. Phys.* **49** 373

[8] Luo J H and Xiao J J 2023 *Chin. Phys. B* **32** 027801

[9] Keldysh L V 1965 *Sov. Phys.-JETP* **20** 1307

[10] Li Q, Tong X M, Morishita T, Wei H and Lin C D 2014 *Phys. Rev. A* **89** 023421

[11] Li Q, Tong X M, Morishita T, Wei H and Lin C D 2014 *J. Phys. B: At. Mol. Opt. Phys.* **47** 204019

[12] Zimmermann H, Patchkovskii S, Ivanov M and Eichmann U 2017 *Phys. Rev. Lett.* **118** 013003

[13] Hu S, Hao X, Lv H, Liu M, Yang T, Xu H, Jin M, Ding D, Li Q and Chen J 2019 *Opt. Express* **27** 31629

[14] Xu S, Liu M, Hu S, Shu Z, Quan W, Xiao Z, Zhou Y, Wei M, Zhao M, Sun R, Wang Y, Hua L, Gong C, Lai X and Chen J 2020 *Phys. Rev. A* **102** 043104

[15] Corkum P 1993 *Phys. Rev. Lett.* **71** 1994

[16] Shvetsov-Shilovski N, Goreslavski S, Popruzhenko S and Becker W 2009 *Laser Phys.* **19** 1550

[17] Landsman A, Pfeiffer A, Hofmann C, Smolarski M, Cirelli C and Keller U 2013 *New J. Phys.* **15** 013001

[18] Huang K, Xia Q and Fu L 2013 *Phys. Rev. A* **87** 033415

[19] Zhao L, Dong J, Lv H, Yang T, Lian Y, Jin M, Xu H, Ding D, Hu S and Chen J 2016 *Phys. Rev. A* **94** 053403

[20] Yun H, Mun J H, Hwang S I, Park S B, Ivanov I A, Nam C H and Kim K T 2018 *Nat. Photon.* **12** 620

[21] Ortmann L, Hofmann C, Ivanov I A and Landsman A S 2021 *Phys. Rev. A* **103** 063112

[22] Venzke J, Reiff R, Xue Z, Jaroń-Becker A and Becker A 2018 *Phys. Rev. A* **98** 043434

[23] Chetty D, Glover R D, deHarak B A, Tong X M, Xu H, Pauly T, Smith N, Hamilton K R, Bartschat K, Ziegel J P, Douguet N, Luiten A N, Light P S, Litvinyuk I V and Sang R T 2020 *Phys. Rev. A* **101** 053402

[24] Chetty D, Glover R D, Tong X M, deHarak B A, Xu H, Haram N, Bartschat K, Palme A J, Luiten A N, Light P S, Litvinyuk I V and Sang R T 2022 *Phys. Rev. Lett.* **128** 173201

[25] Piraux B, Mota-Furtado F, O'Mahony P F, Galstyan A and Popov Yu. V 2017 *Phys. Rev. A* **96** 043403

[26] Harris D O, Engerholm G G and Gwinn W D 1965 *J. Chem. Phys.* **43** 1515

[27] Dickinson A S and Certain P R 1968 *J. Chem. Phys.* **49** 4209

[28] Light J C and Walker R B 1976 *J. Chem. Phys.* **65** 4272

[29] Tong X M and Chu S I 1997 *Chem. Phys.* **217** 119